Lectures given at the NATO Advanced Study Institute *Scale Invariance, Interfaces and Non-Equilibrium Dynamics* June 20-30, 1994, Cambridge, U. K.
Published in *Scale Invariance, Interfaces and Non-Equilibrium Dynamics*
Edited by A. McKane et al, NATO ASI Series B: Physics, Vol. 344, p. 63-83
(Plenum Press, New YorK and London, 1995).

SHAPES AND DYNAMICS OF LAPLACIAN GROWTH

Vincent Hakim

Laboratoire de Physique Statistique
24 rue Lhomond
F–75231 Paris Cedex 05
France

1. INTRODUCTION

Diffusion-limited interface dynamics appears in various physical processes such as crystallisation or aggregation. Plane and spheres are often unstable and non-trivial and sometimes very complex morphologies appear. From a general viewpoint, it is an interesting example of pattern formation out of equilibrium[1] and as such it has been intensely studied[2–5] during the last decade both experimentally and theoretically. In these lectures, we approach the subject by focussing on the dynamics of an interface the motion of which is controlled by a Laplacian field. We start by recalling the classic instability which arises in this context. Surface tension, which regularises the problem at short wavelengths, plays an important role in pattern formation at latter times. When it is anisotropic, the problem is somewhat easier since simple growing shapes can be obtained. The first part of these lectures is devoted to this case. The analysis of shape selection by surface tension is briefly described as well as more recent studies of faceted dendrites, self-affine growing shapes and simplified models of anisotropic growth. To analyse the complex patterns which form in the isotropic case, many paths have been followed by different authors. Singularity dynamics, mean-field theory and averaged patterns as well as some problems concerning the related η-models and Laplacian random walks are visited in the second part.

1.1 Physical models and basic equations

In most physical examples, the interface motion is controlled by a field u describing the diffusion of some conserved quantity,

$$D\nabla^2 u = \partial_t u \tag{1.1}$$

The prototypic examples are crystal growth in a supersaturated solution or in supercooled liquid where the diffusing field are impurity concentration and temperature ('heat conservation'). We limit ourselves here for simplicity to the case where the diffusion takes place in one phase only (the 'one-sided' model). This is rather realistic for impurity diffusion but of course less justified for heat diffusion.

On the interface, there are two boundary conditions. One describes the generation of the diffusing quantity at the interface (due to impurity concentration difference between the solid and liquid phase in the first case (the so-called 'miscibility gap') or latent heat release in the thermal case). It relates the normal velocity of the interface v_n to the normal gradient of the diffusing field:

$$v_n = D\ n.\nabla u \tag{1.2}$$

The other boundary condition fixes the value of the diffusing field at the interface. Namely, the bulk value (the melting temperature) corrected by interface curvature effects due to interfacial energy cost (the 'Gibbs-Thomson effect'):

$$u_{int} = d(\theta)/R \tag{1.3}$$

where R is the local interface radius of curvature.

The surface energy can depend on the orientation of the interface relative to the cristalline axis. This dependence is encoded in the Wulff plot $w(\theta)$ where θ is the angle of the local normal to the interface with a fixed axis (an example of a fourfold anisotropy is $w(\theta) = 1 - \alpha \cos(\theta)$). This dependence appears in the Gibbs-Thomson equation (1.3) as $w(\theta) + w"(\theta)$ ('the surface stress') as can be seen by minimizing $\int ds\ w(\theta)$. Therefore, we write $d(\theta)$ as

$$d(\theta) = d_0\ [w(\theta) + w"(\theta)] \tag{1.4}$$

Important dimensionful quantities in these equations are the 'capillary length' d_0 and for a pattern moving at a velocity v, the 'diffusion length' D/v. The Peclet number $\rho v/D$ measures a characteristic scale of the pattern on the scale of the diffusion length.

In most of these lectures, the Laplacian limit where the time derivative in eq.(1.1) is taken equal to zero will be considered.

$$\nabla^2 \phi = 0 \tag{1.5}$$

$$v_n = n.\nabla\phi \tag{1.6}$$

$$\phi_{int} = \gamma(\theta)/R \tag{1.7}$$

This is usually a good approximation on length scales small compared to the diffusion length but important differences exist between the two cases, some of which will be commented upon as we proceed. It can already be noted that γ has not the dimension of a length as d in eq.(1.3) but has dimension L^3/T. It can be non-dimensioned by a flux Q (rate of area growth) times a characteristic scale of the pattern

Viscous fingering[6] is a simple hydrodynamic example where the Laplacian equation (1.5) is obtained directly and not as an approximation to the diffusion equation (1.1). This describes the motion of the air/oil interface when air is blown into the gap between two close glass plates which has been filled with oil. In this case, ϕ is proportional to the pressure in the oil. Equation(1.5) follows from the fact that the mean oil velocity between the plates is proportional to the gradient of pressure (a local Poiseuille flow) and from oil incompressibility[7].

Equations(1.5-1.7) may usefully be thought of in the following way. At some time t, the interface is known. Then from the first equation (1.5) and the boundary condition (1.7) the field can be computed. Equation (1.6) can then be used to move the interface and find its position at $t + \Delta t$.

The popular DLA model of fractal growth[5] can be thought of as a stochastic way of simulating the equations (1.5-1.7). $\phi(x)$ is then proportional to the probability that a random walker is at x. Since $\phi(x) = 0$ on the aggregate (the absorbing boundary condition), a regularised continuum version cannot involve surface tension. Since sticking of a particle at one point also move the interface at the neighbouring points, an appropriate regularisation may be to modify eq.(1.6) instead, as

$$v_n(s) = \int ds' g(s - s') n.\nabla\phi(s') \tag{1.8}$$

The effect of $g(s)$ is to spread the growth over a small neighbourhood roughly of the size a of a sticking particle. For example, $g(s) = 1/\sqrt{\pi}a \ \exp -(s/a)^2$ can be chosen.

1.2 Instability of a planar front

This is probably the most important basic property of these equations. A moving approximately planar front does not remain planar[6,8] : disturbances grow. It is worth showing this explicitly since the computation is quite simple and instructive.

Let us imagine a viscous fingering experiment. A planar interface $y = y_o(t)$ is moving in the y direction. Its velocity is clearly related to the flux of air which is injected. That is, if the asymptotic behavior of ϕ is prescribed to be $\phi \sim Ay$ then (1.5) and (1.7) imply that $\phi = A(y - y_o(t))$. From (1.6) one then obtains $dy_o(t)/dt = A$ i.e. $y_o(t) = At$.
Now let us consider a small disturbance on the planar interface,

$$y_{int}(t) = y_o(t) + \epsilon(t)\sin(kx), \quad \epsilon << 1 \tag{1.9}$$

This sinusoidal perturbation of the interface will generate a similar perturbation in the field ϕ. Since it satisfies Laplace equation, it will be of the form

$$\phi = A[y - y_o(t)] + \eta(t)\sin(kx)\exp(-ky) \tag{1.10}$$

(remember that the asymptotic behavior is prescribed). Since ϵ and η are small, the value of the field on the interface is at first order

$$\phi_{int} = [A\epsilon(t) + \eta(t)]\sin(kx) \tag{1.11}$$

In the zero surface tension case, ϕ should vanish on the interface and this gives simply $\eta(t) = -A\epsilon(t)$. If surface tension is taken into account, the curvature of the interface to first order in the perturbation is $1/R \simeq -d^2y_{int}/dx^2 = k^2\epsilon\sin(kx)$. Equations (1.7) and (1.11) give

$$\eta(t) = -\epsilon(t)(A - \gamma k^2) \tag{1.12}$$

Now that we have determined ϕ as a function of the interface geometry, we can compute its motion. From (1.9) and (1.10), we obtain to first order,

$$v_n = A + d\epsilon/dt\sin(kx) \tag{1.13}$$
$$n.\nabla\phi = A - k\eta(t)\sin(kx) \tag{1.14}$$

Comparing the two and using (1.12), the evolution of $\epsilon(t)$ is determined

$$d\epsilon/dt = \epsilon(t)k(1 - \frac{\gamma}{A}k^2) \tag{1.15}$$

All perturbations of wavelength smaller than $2\pi\sqrt{\gamma/A}$ are amplified. Without surface tension, the shorter the wavelength the faster the perturbation is growing.

For the DLA-motivated regularisation (1.8), the calculation can be similarly performed. One obtains

$$d\epsilon/dt = \epsilon(t)k \int_{-\infty}^{+\infty} \cos(kx)g(x) \tag{1.16}$$

Two examples are $g(x) = 1/[a\cosh(x/a)]$, which gives for the amplification rate $\sigma_k = k/\cosh(ka\pi/2)$, and $g(x) = 1/\sqrt{\pi}a \ \exp-(x/a)^2$ which gives $\sigma_k = k\exp[-(ka)^2/4]$. Both gives a positive amplification of all wavelengths but with a rate which decreases very fast for k larger than the maximally amplified wavenumber.

2. SIMPLE SHAPES AND SELECTION BY ANISOTROPIC CAPILLARY EFFECTS

A planar front is unstable and that is also true for an expanding circle[2]. Therefore, it is interesting to see whether one can find other simple shapes which would solve the dynamical equation and would hopefully be stable. The first such candidate was found more than fifty years ago by Ivantsov as a model of an advancing dendritic tip.

2.1 The simplest shape : a parabola

Let us consider a shape moving at velocity V along the x-direction taking the diffusion limited case to begin with. Since we intend to look for a pointed solution it is useful to non-dimensionalize lengths by choosing as length unit ρ, its tip radius of curvature. The diffusing field u satisfies the following equations in the reference frame of the interface moving at constant velocity V in the x-direction,

$$\nabla^2 u + Pe\frac{\partial u}{\partial x} = 0 \tag{2.1}$$

$$n.\nabla u = Pe\cos\theta \tag{2.2}$$

$$u_{int} = \frac{d_0}{\rho R}[w(\theta) + \frac{d^2 w}{d\theta^2}] \tag{2.3}$$

The boundary condition at infinity is that u should tend to the undercooling Δ. The Péclet number Pe is the ratio of the tip radius of curvature to the diffusion length $Pe = \rho V/D$.

Ivantsov's remarkable discovery[9] is that these equations have an exact solution, for any Péclet number, when capillary effect are neglected ($d_0 = 0$), with an interface shape which is a simple parabola. The simplest way to verify it is to write the Laplacian in parabolic coordinates[2]. The end result of the calculation is a relation between the undercooling Δ and the Péclet number which reads in the small Péclet number limit

$$\Delta \simeq \sqrt{Pe\,\pi/2} \tag{2.4}$$

This relation determines the product of the tip velocity times the radius of curvature but not the two separately (this is expected since the diffusion constant is the only external dimensionful parameter once the capillary length d_0 has been neglected)

Here, we follow a slightly different path[10]. We first reduce the diffusive case to a Laplacian problem in the small Péclet limit ($Pe << 1$). In this limit, it is easily seen that a parabola is an exact solution of the problem when capillary effects are neglected. Moreover, one also obtains a dimensionless parameter characterizing the magnitude of capillary effects.

In the small Péclet limit where the diffusion length D/V is much larger than the parabola tip radius of curvature, the problem can be decomposed into an asymptotic region, where capillary effects can be neglected, and a tip region. In the neighbourhood of the needle tip, one can take the limit $Pe \to 0$ and solve a Laplacian problem for the field $\phi = \frac{u}{Pe}$ which has a finite nontrivial limit

$$\nabla^2 \phi = 0 \tag{2.5}$$

$$n.\nabla \phi = \cos\theta \tag{2.6}$$

$$\phi_{int} = \frac{\sigma}{R}[w(\theta) + \frac{d^2 w}{d\theta^2}] \tag{2.7}$$

This reduced Laplacian problem depends on the single parameter[11] $\sigma = d_0/(\rho Pe)$. It has a solution only for special values of σ which are thus a kind of nonlinear eigenvalues[10]. The velocity V and length scale ρ are completely determined once the Ivantsov relation (2.4) for the asymptotic parabola is taken into account.

Let us now see how the reduced problem (2.5-2.6) can be analysed. As we will find many times in these lectures, it is useful to transform the moving free boundary problem into a problem with conditions on a known boundary by changing variables.The interface is a line of flow in a fluid mechanical analogy. That is, one has $\psi = y$ on the interface[12]. So, the interface is located on the real axis of the complex $\hat{\omega}$-plane where $\hat{\omega} = \hat{\phi} + i\hat{\psi} = \phi + i\psi - (x + iy)$ is the complex velocity potential in the reference frame of the moving interface. In these coordinates, the free boundary problem is transformed in the more easily tackled problem of finding $z = x + iy$ as a function of $\hat{\omega}$. It is instructive to see first how the Ivantsov parabolic needle crystal ($\sigma = 0$) is obtained in this framework. In this case, $z(\hat{\omega})$ is such that:

i) $z(\hat{\omega})$ should be an analytic function of $\hat{\omega}$,

ii) on the positive real $\hat{\omega}$ axis, $x = -\hat{\phi}$ (since $\phi = 0$ on the interface),

iii) $z(\hat{\omega})$ should grow linearly at infinity and not faster so as to obtain an univalued complex potential,

iv) the only allowed singularities of $z(\hat{\omega})$ are located where the velocity $\frac{d\hat{\omega}}{dz}^*$ vanishes in the moving interface frame, that is at the needle tip $\hat{\omega} = 0$. In order to obtain a smooth interface shape when going around $\hat{\omega} = 0$ from the lower real axis to the upper real axis this should be a square root singularity (to transform the 2π turn into a normal tangent).

The solution is simply

$$z(\hat{\omega}) = -\hat{\omega} + ia\sqrt{\hat{\omega}} \tag{2.8}$$

where a is a constant that we choose to be real. On the real positive $\hat{\omega}$-axis this gives the classical parabolic shape $x = -\hat{\phi}, y = \pm a\sqrt{\hat{\phi}}$. a should be taken equal to $\sqrt{2}$ to agree with our previous choice of length normalisation.

For finite σ, it is convenient to first determine the derivative $v \equiv \frac{d\hat{\omega}}{dz}$ (the complex conjugate of the complex velocity) as a function of the complex potential $\hat{\omega}$. We search for a shape symmetric about the velocity axis (the x-axis) and write the equations[13] for a half-profile. Denoting by α, the angle between the interface tangent and the velocity axis, υ can be written as

$$\upsilon = -q \exp(i\alpha) \tag{2.9}$$

The analytic function υ can be determined from the relations it satisfies on the real axis. When the curvilinear abscissa $s = -\infty$, $\alpha = 0$ and at the interface tip $s = 0$,$\alpha = -\pi/2$. The x-axis in front of the advancing interface is a streamline so $\hat{\psi} = 0$, $\alpha = 0$ there. On the remaining portion of the $(\hat{\psi} = 0)$-axis (i.e. along the interface), the modulus q and the argument α of the analytic function $q\exp(-i\alpha)$ are related as follows. Using,

$$\frac{d}{ds} = \frac{d\hat{\phi}}{ds}\frac{d}{d\hat{\phi}} = -q\frac{d}{d\hat{\phi}} \tag{2.10}$$

one obtains

$$\phi = \frac{\sigma}{R} \Rightarrow \hat{\phi} = -\sigma\frac{d\alpha}{ds} - x = \sigma\ q\ \frac{d\alpha}{d\hat{\phi}} - x \tag{2.11}$$

x can be eliminated by differentiating once more with respect to s, and one obtains along the real $\hat{\phi}$-axis

$$\sigma\ q\frac{d}{d\hat{\phi}}q\frac{d\alpha}{d\hat{\phi}} - q = -\cos(\alpha) \tag{2.12}$$

Unfortunately, we do not know how to obtain υ analytically using this equation. Two kinds of approaches have been followed instead:

- One can determine υ numerically[13,14,3] from eq.(2.12) or analogous equations. The main result is that the problem has no solutions when surface tension is isotropic. It is impossible to satisfy all the boundary conditions. If surface tension is anisotropic then solutions are obtained for a discrete number of values of σ, ($\sigma = \sigma_n,\ n = 0, 1, ...$). One convincing way of showing it is to relax one boundary condition so that the problem is not overdetermined and can be solved for any value of σ. Then one can select from the obtained solutions those which satisfy the relaxed condition. For example if $\alpha(0) = -\pi/2$ is not imposed at the start, one can compute $\alpha(0)$ as a function of σ[14]. With anisotropy, $\alpha(0)$ turns out to be a function of σ which oscillates around $\pi/2$ and each crossing corresponds to a solution of the problem.
- In the small σ limit, one can analyse the problem starting from the exact Ivantsov solution at $\sigma = 0$. This turns out to be more subtle than it can first be guessed as we briefly explain below.

2.2 Capillary effects and selection

When surface tension is treated as a regular perturbation, no particular effect is noticed and no value of σ seems to be selected. The difficulty is more easily understood on a simple ordinary differential equation[3,15] (see ref.[16] for other examples) ,

$$\sigma\frac{d^3\theta}{dz^3} + \frac{d\theta}{dz} = \cos\theta \tag{2.13}$$

In (2.13), θ may be interpreted as an angle between the normal of an interface and the propagation axis and σ may be viewed as above as quantifying the importance of capillary effects. So, a symmetric shape corresponds to an odd function $\theta(z)$ with the boundary conditions $\theta(-\infty)=-\pi/2,\ \ \theta(+\infty)=\pi/2$.

For $\sigma=0$, equation (2.13) is easily solved (a simple analog of Ivantsov's result)

$$\theta_0=-\frac{\pi}{2}+2\arctan(e^z), \tag{2.14}$$

Successive terms in a perturbation expansion can also be computed. Writing $\theta=\theta_0+\sigma\theta_1+...$, one obtains

$$\theta_1=-\frac{z}{\cosh z}+2\frac{\sinh z}{\cosh^2 z},... \tag{2.15}$$

It is not difficult to see that successive terms of the perturbation expansion can be obtained to any order, that they are odd in z and satisfy the required boundary conditions. So, a regular perturbation expansion does not give any obvious hint on the problem overdetermination.

However, a simple counting of diverging modes at infinity makes it plausible that the boundary conditions $\theta(\pm\infty)=\pm\pi/2$ are too stringent to be imposed at the same time. There are two divergent modes and one convergent mode around $z=-\infty$ and $z=+\infty$. But eq. (2.13) is a third order equation and its solution only depends on three arbitrary constants. If we start the integration at $z=-\infty$, two constants are fixed by the annulation of the two diverging modes at $z=-\infty$ and, one constant is missing to kill the two diverging modes at $z=+\infty$. In a similar way, once the two diverging modes at $z=-\infty$ have been killed, one can use the last constant to choose $\theta(0)=0$. There is then no reason for $\theta''(0)$ to vanish and the solution to be odd.

What goes wrong with the simple perturbation expansion is that the non-existence of the solution comes from exponentially small effects. The asymptotic behavior of $\theta''(0)$ as σ tends to zero is

$$\frac{d^2\theta}{dz^2}|_{\theta=0}\simeq\frac{2\Gamma}{\sigma^{5/4}}\exp(-\frac{\pi}{2\sqrt{\sigma}}) \tag{2.16}$$

This vanishes to every finite order in σ and some care must be exercised to obtain this asymptotic behavior. The main classic idea is that the small parameter σ multiplies the highest derivative in eq. (2.13) and cannot be neglected in a region of rapid variation of the function $\theta(z)$ (a 'boundary layer'). Here however, there is no such region for real value of z and one should resum the perturbation expansion around a complex singularity of the terms of the perturbation expansion[15,17]; $\pi/2$ in the argument of the exponentially small term comes from the location of the dominant singularities $z=\pm i\pi/2$. The effect of anisotropy can be mimicked in this simple example by multiplying the highest derivative term in eq.(2.13) by a function of θ such as $[1-\epsilon\cos(\theta)]$. The prefactor of the exponentially small term in eq.(2.13) becomes a function $\Gamma(\epsilon,\sigma)$ of ϵ and σ and its zeroes give the selected values $\sigma_n(\epsilon)$.

An analogous strategy can be used to analyse the reduced Laplacian problem for small σ[18−20,3]. From the above parabolic solution, one obtains

$$\frac{dz}{d\hat{\omega}}=-1+i\frac{1}{\sqrt{2\hat{\omega}}}\Rightarrow\frac{d\hat{\omega}}{dz}=\frac{\sqrt{2\hat{\omega}}}{-\sqrt{2\hat{\omega}}+i}=-q_0\exp(i\alpha_0) \tag{2.17}$$

Therefore

$$q_0=\sqrt{\frac{\hat{\omega}}{\hat{\omega}+1/2}} \tag{2.18}$$

Near the singularity of q_0, $\omega = -1/2$, the perturbation expansion can be resummed by introducing rescaled variables,

$$q \sim -i\sigma^{-1/7} G, \quad \xi \sim \sigma^{2/7}(\omega + 1/2) \tag{2.19}$$

In these new variables, Eq.(2.12) reduces to lowest order in σ to the (inner) problem,

$$\frac{d^2 G}{d\xi^2} + \frac{1}{G^2} = \xi \tag{2.20}$$

the solution of which give the lowest term of the resummed expansion. The requirement that q is odd imposes that q is purely imaginary on the real negative $\hat{\omega}$- axis near the origin or, equivalently, that G is real for positive ξ. When there is no anisotropy of surface tension no such solution is found. With anisotropy[3,19,20] the inner problem is modified and as in the simple example above a discrete (infinite) number of solutions is found such that $\sigma \sim \epsilon^{+7/4}$. It can moreover be shown[21,22,3], in accordance with the numerics[23] that all solutions except the lowest one are unstable.

2.3 Faceted dendrites

In the previous section, we have seen that a small and smooth capillary anisotropy plays a very important role in the dynamics of dendritic growth. The case of dendrites growing below the roughening temperature is also interesting. In some experiments[24], faceted dendrites have been observed. The approach described above has recently been adapted to this case. We will consider as before the two-dimensional case for simplicity.

Firstly, in the faceted case, $w(\theta)$ has a conic point for some specific direction θ_f with two different derivatives $dw/d\theta \mid_+$ and $dw/d\theta \mid_-$ and eq.(1.7) is obviously ill defined there. Moreover, since the geometry of the facet is known, one cannot impose both conditions (1.6) (a Neumann condition) and (1.7) (a Dirichlet condition) on the Laplacian field. On the facet, it appears necessary to keep eq.(1.6) which is a conservation equation and to find a single condition replacing (1.7) and determining the facet length (its only geometric unknown). Neglecting kinetic effects, this condition[25,26] can be very simply obtained[27], by imagining the conic point as the limit of more and more peaked smooth anisotropies for which eq.(1.7) is still valid. Then, averaging eq.(1.7) in the region of rapid variation gives (recalling that $1/R = -d\theta/ds$)

$$\int_{facet} ds\ \phi_{int} = \sigma[dw/d\theta \mid_+ - dw/d\theta \mid_-] \tag{2.21}$$

where the integration is taken over the facet length. On the facet, this single condition on the average field replaces the local Gibbs-Thomson condition on the facet. Therefore, the determination of a faceted needle crystal is a mixed problem where the interface geometry is unknown but the field is known (eq.(1.7)) on the rough parts of the interface while the inverse is true on the facets.

In order to analyse this problem, a strategy similar to the one used for the classical rough case has been followed[28]. A 'zero-surface tension' case is obtained by neglecting surface tension on the rough parts. That is, eq.(1.7) is replaced by $\phi = 0$ on the rough parts but one still requires that the shape has facets of length L normal to the directions $\pm\theta_f$. It is still true that the interface is a streamline in its moving frame. As above, one can therefore search to determine z as a function of the complex velocity potential $\hat{\omega}$. It is again more convenient to determine first the derivative $\chi \equiv \frac{dz}{d\hat{\omega}}$. It is parallel to the complex velocity $(\frac{d\hat{\omega}}{dz}^*)$ so, on the facets

$$\chi_1 = \pm \tan(\theta_f)\chi_2 \tag{2.22}$$

The requirements on $\chi(\hat{\omega})$ are easily written :

i) χ is analytic in the $\hat{\omega}$-plane cut along the real positive axis.

ii) $\chi_1 = -1$ on the positive real $\hat{\omega}$-axis outside the segment $[\phi_1, \phi_2]$ corresponding to the facet. Equation(2.22) should be satisfied on the facets, the plus (minus) sign holding on the upper (lower) part of $[\phi_1, \phi_2]$.

iii) χ should tend to a constant as $\hat{\omega} \to \infty$

iv) χ has an inverse square root singularity at the origin $\hat{\omega} = 0$.

Finding χ is the classical problem of determining an analytical function given a linear relation between its real and imaginary parts on the real line. It can be solved following standard techniques (see e.g.[29]). The solution reads,

$$\chi = -1 + \frac{i}{Y(\hat{\omega})} \left\{ a\sqrt{\hat{\omega}} + \frac{b}{\sqrt{\hat{\omega}}} - \cos\theta_f \; \Omega \int_{f_1}^{f_2} \frac{df}{\pi\sqrt{f}} \frac{Y_r(f)}{f - \hat{\omega}} \right\} \tag{2.23}$$

with

$$Y(\hat{\omega}) = (\omega - f_1)^{1-\theta_f/\pi} (\hat{\omega} - f_2)^{\theta_f/\pi}, Y_r(\hat{\omega}) = (\hat{\omega} - f_1)^{1-\theta_f/\pi} (f_2 - \hat{\omega})^{\theta_f/\pi} \tag{2.24}$$

The determination of $Y(\hat{\omega})$ is chosen such that it is real positive for $\hat{\omega}$ real and larger than f_2. Separating real and imaginary parts of eq. (2.23) on the real $\hat{\omega}$-axis, a parametric description of a faceted dendrite is obtained. The constants a and b in eq.(2.23) can be fixed by imposing that the facets and rough part match tangentially as required when there are no missing orientations in the Wulff plot. Shapes with different facet lengths are plotted in fig.1.

However, eq.(2.23) is not a satisfactory solution of the zero-surface tension problem as posed above. Fortunately, a slight modification of it seems to cure its defect and solve the surface tension selection question at once! The problem comes from the fact that, for determining the shape, the condition on the rough parts $\hat{\phi} = -x$ (i.e. $\phi = 0$) has been replaced by $dx/d\hat{\phi} = -1$. In the usual rough case, this is a harmless change. But here, the front and trailing rough parts are not contiguous. Although ϕ is constant on each of them, the value of the constant differs between the front and trailing rough parts. If ϕ is chosen equal to zero on the trailing rough parts, a positive value ϕ_{front} for ϕ is obtained on the front rough part[30]. So, the zero-surface tension problem as originally posed has no solutions. Suppose instead that σ, which measures capillary effect on length scales characteristic of the asymptotic parabola, is small but finite. That has a weak effect on the trailing parts but it can play a strong role for a strongly curved front part. This can be taken advantage of, in the limit of long facets almost reaching the dendrite tip. The exact but unphysical 'zero surface tension' solution can be transformed into an approximate but satisfactory solution, by simply replacing its small front rough part by an arc of circle. This small shape modification does not modify much the diffusing field but the unphysical undercooling of the front part can now simply be attributed to capillary effects,

$$\phi_{front} = \frac{\sigma}{R_{front}} \tag{2.25}$$

Since the radius of the front rough part is geometrically related to the ordinate y_{front} of the facet front extremity $R_{front} = y_{front}/\sin(\theta_f)$, eq.(2.25) can be rewritten as

$$\sigma = \frac{y_{front}\;\phi_{front}}{\sin(\theta_f)} \tag{2.26}$$

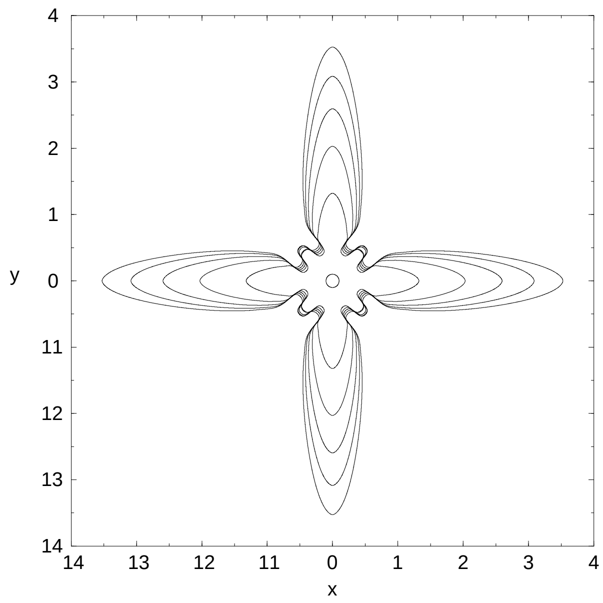

Figure 1. $\epsilon = 0.5$, $\gamma_0 = 0.001$, $t = 0$ to 1.5, $\Delta t = 0.3$

In the large facet length limit, the capillary parameter σ is therefore entirely selected by quantities computed using the zero-surface tension solution (2.23) in the large facet length limit (the facet length should of course be related to the magnitude of the slope discontinuity in the Wulff plot using eq.(2.21). This simple selection scenario seems to be qualitatively confirmed by recent numerics[31] but precise results in the limit of large facets are still needed for a detailed comparison.

2.4 Anisotropy and self-affine growth

From the previous sections, the reader may have gained the impression that with anisotropy the dendritic tips move at constant speed in Laplacian growth. This is the case in the diffusive setting (1.1) but for a pure Laplacian field, one does not have Ivantsov's relation (2.4) and the above is certainly not the complete story. What happens in this latter case has been clarified recently[32].

Fig.1 shows a computer simulation of eq(1.5-1.7) where γ has a four-fold anisotropy $\gamma(\theta) = \gamma_0[1 - \epsilon\cos(4\theta)]$. The angle θ is the orientation of the outward normal relative to a fixed direction and γ_0 is a constant. What the numerics shows is that the tips of the main branches do not move at a fixed velocity. Their length L is found to grow like t^α with $\alpha = .60$. Similarly, their width w grows like t^β with $\beta = .40$. The shapes at different times can actually be superimposed by rescaling their lengths and widths as shown in Fig.2.

These observations can be understood easily, using the results of the previous sections. Here, Ivantsov's relation is simply replaced by the fact that the asymptotic behavior of the field is

$$\phi \sim Q/2\pi \ \ln(r) \tag{2.27}$$

(in the following, we choose $Q = 2\pi$). Flux conservation implies that the area enclosed by the interface grows linearly in time ('air is injected at a constant rate'). The product of a branch length times its width scales like its area. Therefore $L\ w \sim t$ and

$$\alpha + \beta = 1 \tag{2.28}$$

Another relation is obtained by considering the tip dynamics. γ_0 is the only dimensional parameter which controls the selection of the tip shape. As already mentioned, it has the

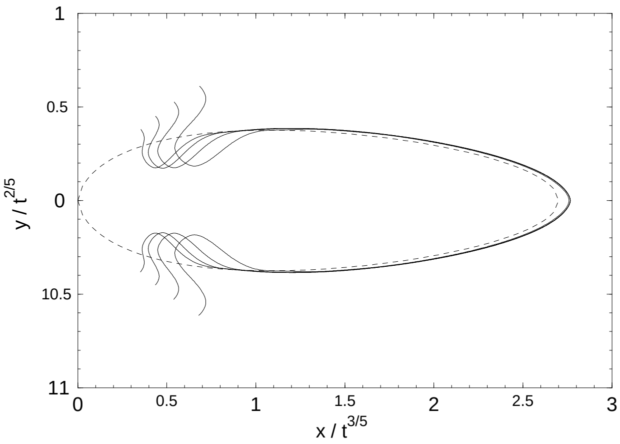

Figure 2. Scaled $\epsilon = 0.5$, $\gamma_0 = 0.001$, $t = 0.6$ to 1.5, $\Delta t = 0.3$.

dimension L^3/T (ϕ, being a rate of change of area, has dimension L^2/T). Therefore, as above the result of selection theory applied to the tip must be a law giving the dimensionless number $\rho^2 V/\gamma_0$ as a function of the anisotropy ϵ, where ρ denotes the tip radius of curvature and V its instantaneous velocity. Since $V \sim dx/dt \sim t^{\alpha-1}$ and $\rho \sim (d^2x/dy^2)^{-1} \sim t^{2\beta-\alpha}$, we see $\rho^2 V \sim t^{4\beta-\alpha+1}$, and constancy of $\rho^2 V$ requires

$$\alpha - 4\beta = 1 \tag{2.29}$$

Comparing (2.28) and (2.29) one obtains $\alpha = 3/5, \beta = 2/5$ in agreement with the numerics.

A simple calculation[33,32]also gives the growing self-similar shape of Fig.2. At large times, since the width of each growing arm becomes small compared to its length, each branch may be approximated by a line segment and the overall shape by a cross. Moreover since the curvature of a branch is small except in the immediate neighbourhood of its tip, ϕ can be taken to be zero on the segments. The advantage of doing this, is that one can then explicitly compute the field ϕ. The general idea is to transform the cross by an analytic transformation into a shape for which the problem is easy to solve. The solution around the cross is then obtained by composing the mappings. Using complex notations, the z-plane ($z = x + iy$) outside a cross with vertices at $\pm L(t)$, $\pm iL(t)$, is mapped onto the outside of the unit disk in a ξ-plane by,

$$z = \frac{L(t)}{\sqrt{2}}(\xi^2 + \xi^{-2})^{1/2} \tag{2.30}$$

In the ξ-plane, the Laplacian field $\phi(\xi)$, with $\phi = 0$ on the surface of the disk and having the far-field behavior (2.27), is simply

$$\phi = \ln(r) = Re[\ln(\xi)] \tag{2.31}$$

The field around the cross is immediately obtained as

$$\phi = Re[\ln(\xi(z))] \tag{2.32}$$

since it satisfies the right boundary conditions by construction and is an harmonic function as the real part of an analytic function. Knowing the field ϕ, the branch shape can now be determined. The lateral velocity at a point x along the rightward-growing branch is given by the y-derivative of the potential (2.32) as

$$\frac{dy}{dt} = \frac{x}{\sqrt{L(t)^4 - x^4}}, \qquad 0 < x < L(t) = At^{3/5}.$$

The complete asymptotic shape is therefore

$$y(x,t) = t^{2/5} \frac{5}{3A} \left(\frac{x}{L(t)} \right)^{2/3} \int_{x/L(t)}^{1} \frac{ds}{s^{2/3}\sqrt{1-s^4}}. \tag{2.33}$$

The remaining parameter A can be determined by using the previously explained determination of tip dynamics by capillary effects

$$\frac{\gamma_0}{\rho(t)^2\, V(t)} = \sigma(\epsilon) \tag{2.34}$$

Since $\rho = \frac{1}{2}(5/3)^2 A^{-3} t^{1/5}$ and $V = (3/5)At^{-2/5}$, one obtains

$$A(\epsilon) = \left(\frac{125\sigma(\epsilon)}{108\,\gamma_0} \right)^{1/5}.$$

For the simulation value $\gamma_0 = .001$, $A(0.5) = 2.70$ is obtained, using[19,3] $\sigma(0.5) = .124$. The obtained dashed analytical curve (2.33) agrees well with the numerical results as shown in Fig.2.

An ingenious use of these two dimensional growing shapes has been recently suggested for the computation of steady three-dimensional dendritic tips with cubic anisotropy[34].

2.5 Anisotropic dynamics in a simplified setting: the needle models

In the previous section, an accurate description of growing anisotropic branches has been obtained by replacing them by simple needles. It is tempting to push this simple model one step further in order to study the relative dynamics of different branches and the competition between them. For example, a simple question that can be considered is to determine when n-fold anisotropy produces a n-fold symmetric pattern of growing branches[35]. A more complicated problem is to analyse the coarsening properties of an array of branches[36]. In order to deal with these questions, the above simple needle model can be extended as follows[35]. We consider n needles growing from a common center along fixed directions in the plane. The field ϕ which controls the growth of the needles is supposed to satisfy Laplace's equation, it is chosen to be zero on the needles and grows like $\log(r)$ at large distance r from the center. These boundary conditions and Laplace's equation determine ϕ completely for a given geometry of needles. Along the k-th needle, at a small distance r from its tip r_k, the gradient of ϕ behaves like $r^{-1/2}$

$$\left| \vec{\nabla}\phi(r + r_k) \right| \sim \frac{E_k}{\sqrt{r}} \tag{2.35}$$

A family of possible dynamics (characterized by the exponent η) is introduced in this simplified model by requiring that the growth velocity of a needle be proportional to E_k to the power η ('the flux on the k-th tip'),

$$\frac{dl_k}{dt} = E_k^{\eta} \tag{2.36}$$

where l_k denotes the length of the k-th needle.

In order to study this model analytically one needs to compute the field ϕ . As above, this is conveniently done by finding a conformal transformation which maps the exterior of the unit disk (ξ-plane) onto the exterior of the star-shaped object formed by the n needles (z-plane). Such a transformation is for example,

$$z = f(\xi) = A\,\xi \prod_{j=1}^{n} \left(1 - \frac{e^{i\theta_j}}{\xi}\right)^{\alpha_j}, \quad \sum_{j=1}^{n} \alpha_j = 2 \tag{2.37}$$

The α_j are fixed parameters given by the angles $\alpha_j \pi$ between the successive needles.

Instead of studying the general case, we choose here to illustrate the technique with the simple example of an even number n of needles growing in directions spaced regularly at relative angles of $2\pi/n$ (i.e. $\alpha_j = 2/n$). For $n > n_c(\eta)$ the symmetry between the n growing needles is spontaneously broken. This may be seen as follows. As usual for the Mullins-Sekerka instability (see section1.2) the shortest wavelength mode is the most dangerous. So we study a shape with needles of alternate lengths $\ell_1 = \ell_3 = ... = L$, $\ell_2 = \ell_4 = ... = l$ using the following mapping

$$z = f(\xi) = \left(\frac{\xi^{n/2} + \xi^{-n/2}}{2} + a\right)^{2/n} \tag{2.38}$$

(a is real and $|a| < 1$). The two values of the lengths L and l are then

$$L = (1+a)^{2/n} \quad \text{and} \quad l = (1-a)^{2/n}$$

whereas the two values of the fields $E \propto |f''(z_i)|^{-1/2}$ at the tips are

$$E_L \propto (1+a)^{1/2-1/n} \quad , \quad E_l \propto (1-a)^{1/2-1/n} \quad \text{and} \quad \frac{E_l}{E_L} = (\frac{l}{L})^{(n-2)/4}$$

Therefore the dynamics for the ratio $R = l/L$ is

$$L\frac{dR}{dL} = R^{(n-2)\eta/4} - R \tag{2.39}$$

So, the fixed point $R = 1$ is unstable and the symmetry between the n growing branches is spontaneously broken for $n > n_c = 2 + (4/\eta)$. For an odd number of branches, the analogous condition for instability is[35] $\eta > \frac{4n}{n^2-2n-1}$.

Up to this point, the exponent η has been considered as an arbitrary model parameter. One can wonder which value of η corresponds to anisotropic Laplacian growth. The coefficient E in (2.35) has dimension $L^{3/2}/T$. So, when expressed in terms of quantities characteristic of the tip dynamics it is proportional to

$$E \sim \rho^{1/2} V \tag{2.40}$$

Comparing this with eq.(2.34), one obtains that the tip velocity V is proportional to $E^{4/3}$. Therefore, one obtains that η in eq.(2.36) is equal to 4/3 for anisotropic Laplacian growth. Together with the previous stability calculation, this predicts that a pattern with six growing branches is actually instable in the sixfold anisotropy case. A numerical (or experimental) test of this conclusion would be welcome.

3. ISOTROPIC RADIAL GROWTH, STOCHASTIC MODELS AND FRACTALS

In the fully isotropic case, experiments show that the interface becomes more and more complex as it moves. This also seems to happen when the motion of an interface obeying equations (1.5-1.7) is simulated and this actually limits the computation to the first few ramifications. In order to study the asymptotic properties of the patterns, simpler stochastic models have been invented and simulated, the prototypic example being the well-known DLA fractals. The properties of radial viscous fingering patterns and diffusion-limited aggregates seem to agree[37].

Various techniques have been proposed and used to study these patterns. We restrict ourselves to analyses of the dynamics[38]. The remarkable properties of the deterministic interface evolution equations (1.5-1.7) are outlined first. Then, mean-field like attempts are described as well as some of the encountered problems. Finally, the reader's attention is drawn to generalised models ('η-models') and to a recent suggestion that they can become simpler for large η.

3.1 Conformal transformation in two dimensions and singularity dynamics

One difficulty of Laplacian growth is that the Laplacian field which controls the motion of the interface depends on a complicated way on the interface geometry. In two dimensions this can be simplified somewhat by using conformal transformations[39–41]. The basic idea is to map conformally the interface on a simple region, a circle say. If capillary effects are neglected, the Laplacian field takes a constant value on the interface and Laplace equation with this simple (Dirichlet) boundary condition can be easily solved in the new geometry. Using the inverse mapping, the Laplace field is then determined around the moving interface. The method can be used to reduce the motion of the interface to the dynamics of a conserved number of complex singularities described by coupled ordinary differential equations. This is a nice mathematical result which is described in subsection 4.1. However, as already seen in the previous sections, capillary effects cannot be neglected if one does not want to restrict oneself to the short time evolution of the interface. In the present context, this is seen quite dramatically since singularities appear in a finite time on the interface for a general initial condition. When capillary effects are taken into account, the Laplacian field is no longer constant on the interface and the method looses much of its simplicity. One hope is that when the capillary number is small, many features of the singularity motions are still partially described by the zero-surface tension dynamics. We briefly describe some of the few results which have been obtained along these lines. The most interesting conclusion at present is perhaps that large departures from the shapes with zero-surface tension can exist before any large curvature appear on the interface shape, contrary to naive expectations.

3.1.1 The zero surface tension case Let us consider an interface moving in a Laplacian field. As for the determination of steady shapes, it is useful to transform the moving free boundary problem into a problem with conditions on a known boundary. In the zero-surface tension case, the simplest way of achieving this is to change variables. Instead of computing the field ϕ as a function of the coordinates (x, y) we introduce the complex velocity potential $W = \phi + i\psi$ and compute $z = x + iy$ as an analytic function of W. The interface is simply located on the line $\phi = 0$ in this new sytem of coordinates (from eq. 1.7). The kinematic conservation equation 1.6 can also be simply written in the (ϕ, ψ)-coordinate system. One has for the interface tangent $\vec{t}$ and normals $\vec{n}$,

$$\vec{t} \propto \frac{\partial z}{\partial \psi} = -i\frac{dz}{dW}, \quad \vec{n} \propto \frac{dz}{dW} \tag{3.1}$$

The field gradient can be written

$$\nabla\phi = (\frac{dW}{dz})^* \tag{3.2}$$

So remembering that the scalar product of two vector $\vec{a}.\vec{b}$ is $Re(ab*)$ in complex notation one obtains for eq.1.6

$$Re[\frac{dz}{dt}(\frac{dz}{dW})^*] = Re[(\frac{dW}{dz})^*(\frac{dz}{dW})^*] = 1 \tag{3.3}$$

Without surface tension the whole problem is reduced to this very simple equation of motion. Given an analytic function $z(W)$, one should evolve it in time keeping $z(W)$ analytic and such that the condition 3.3 is satisfied at all times.

Before trying to solve this for simple initial conditions, we should be more precise on the geometry we are considering and on the boundary conditions on ϕ. For definiteness, we choose a radial geometry and fix the asymptotic behavior of the ϕ-field at infinity to be $\phi \sim Q/2\pi \ln(|z|)$ (which corresponds to injecting air at a fixed flux Q in a viscous fingering experiment). One way to impose this is to define a variable ξ by

$$W = Q/(2\pi)\ln(\xi) \tag{3.4}$$

In the ξ- variable the interface equation of motion reads

$$Re[\frac{dz}{dt}(\xi\frac{dz}{d\xi})^*] = \frac{Q}{2\pi} \tag{3.5}$$

In the ξ-plane the interface is simply the unit disk and at infinity one has $z \sim \xi$. In other words, $z(\xi)$ is a conformal transformation which maps the unit disk of a mathematical ξ-plane onto the interface $z(\xi)$, the exterior of the ξ-disk being mapped onto the region of the physical z-plane where the Laplacian field is defined (the viscous fluid region in viscous fingering). It is also possible to proceed in the reverse way by asserting on general grounds the existence of such a conformal transformation. Then, in the ξ-plane one can immediately determine the Laplacian field which is zero on the interface and has a given logarithmic growth at infinity. It is simply the real part of $W(\xi)$ given by 3.4. The Laplacian field in the physical z-plane is simply given by $\phi = Re(W[\xi(z)])$ as in (2.32). Expressing eq.1.6 in the ξ-variable gives back the equation of motion 3.5.

A simple example illustrates the use of (3.5). We choose

$$z(\xi) = a(\xi + \frac{b}{\xi^n}) \tag{3.6}$$

At $t = 0$, b is supposed to be small ($b(0) << 1$) so that the shape is close to a circle. Now, using equation (3.5) we can compute exactly the non-linear evolution of this shape. Reporting (3.6) in (3.5) one obtains that the form (3.6) is conserved and that a and b satisfy the two evolution equations

$$a^2(t) = \frac{tQ/\pi + a^2(0)[1 - nb^2(0)]}{1 - nb^2(t)} \tag{3.7}$$

$$b(t) = b(0)[a(t)/a(0)]^{n-1} \tag{3.8}$$

For $n = 1$, one obtains an ellipse which grows in time while preserving its shape. However for $n > 1$, the evolution equation for a shows that a begins to grow but reaches its maximum value at a finite t^* when $[a(t)/a(0)]^{n-1} = 1/b(0)\sqrt{n}$ i.e. exactly when b(t) first reaches $1/\sqrt{n}$. That is, when the zeroes of $dz/d\xi$ which were previously located inside the unit ξ-circle first touch it. At such a point the interface is no longer smooth (locally $z(\xi) = z(\xi_0) + \alpha(\xi - \xi_0)^2 + ...$ and a local expansion along the unit circle shows that the singularity is a 2/3 power cusp).

This simple example can be generalized to more general initial conditions. For an initial condition such that $dz_0/d\xi$ is a general polynomial in $1/\xi$ instead of the simple symmetric form (3.6) , it is not difficult to show that singularities appear in finite time[41]. Explicit equations for the motion of the zeroes of $P(\xi)$ can also be obtained[40]. This can be generalised to initial condition which are rational functions of $1/\xi$. In this case poles do not hit the unit circle and there exist cases in which the solution remains valid for all times (for examples see[41]). Conserved form of solutions with more general singularity structure do not appear to be known. For example, it would be interesting to find a smooth interface with n-fold symmetry which tends asymptotically to a shape formed by n growing self-dilating fingers of the type described in[43].

One last result which is worth mentioning is that one can construct an infinity of conserved quantities in the zero surface tension case[42]. These read,

$$C_N = \int_c \overline{z} z^{-N} \tag{3.9}$$

where the integral is along the interface. Changing the integration variable to ξ, differentiating with respect to time and using the evolution equation 3.5, it is not difficult to check that $dC_N/dt = 0$ for $N \geq 1$ while dC_0/dt is constant (reflecting the linear growth of the enclosed area).

3.1.2 Influence of surface tension The appearance of singularities in finite time is clearly due to the fact that short wavelengths are unstable and capillary effects should prevent this from happening[44]. Moreover, taking surface tension into account is clearly needed given its strong influence in determining the large time behavior of the problem as can already be seen at the steady state level. One might hope to understand the dynamics for small surface tension by exploiting the simplicity and remarkable properties of the zero-surface tension dynamics. This program is far from being realized but some progress has been made in understanding how surface tension influences singularity dynamics and how it prevents the appearance of cusps on the interface.

When capillary effects are taken into account (eq.1.7), the conformal transformation $z(\xi)$ (which maps the ξ unit circle onto the interface) is no longer simply related to the complex velocity potential and the two should be determined simultaneously. The interface normal is given as $\vec{n} \propto \xi \frac{dz}{d\xi}$ and the field gradient by (3.2). So, eq.(3.3) can be written as,

$$Re[\frac{dz}{dt}(\xi\frac{dz}{d\xi})^* - \xi\frac{dW}{d\xi}] = 0 \tag{3.10}$$

Equation (1.7) gives another relation between W and z on the interface (i.e. on the unit ξ-circle),

$$Re[W(\xi)] = \frac{\gamma}{|\frac{dz}{d\xi}|}[1 + Re(\xi\ \frac{\frac{d^2z}{d\xi^2}}{\frac{dz}{d\xi}})] \tag{3.11}$$

The analytic functions $W(\xi)$ and $z(\xi)$ are determined by these two relations together with the large-ξ asymptotic behaviours $W \approx Q/(2\pi)\ln(\xi)$, $z \approx a(t)\xi$.

In order to determine the influence of small capillary effects on the interface motion, these equations were solved numerically in ref.[45] starting for simple initial conditions like (3.6). Little modifications were observed when starting with symmetric functions $dz/d\xi$ with poles which do not develop singularities. Although it is clear that surface has an influence on the asymptotic state since it selects one among a family of steady states (here the self-dilating finger of ref.[43]) a longer integration time would presumably be needed to observe it. More remarkable results were obtained with initial conditions which develop singularities in absence of surface tension. As expected, surface tension prevented singularity, but more interestingly, it had a significant influence on the interface shape before the appearance of any large curvature on the zero-surface tension shape contrary to naive expectations. Approximate reconstructions of the solution singularity structure seem to show that the initial zeroes of $dz/d\xi$ emit secondary singularities under the influence of capillary effects. These singularities reach the vicinity of the unit ξ-circle (and therefore modify the interface shape) before the initial zero. Some analytic results in support of this picture have been obtained in ref.[46]. By a local analysis around a singularity in the ξ-disk, it is found that the singularity structure of both poles and zeroes is modified. For an initial pole, the modifications remains limited to a neighbourhood of the singularity for arbitrarily large times as capillary effect tend to zero. On the contrary, the emitted singularities spread away at finite velocities even in the limit where capillary effects tend to zero.

These results are, of course, still quite limited. The appealing goal of understanding the properties of the complex interface shapes as those of a gas of singularities remains to be attained.

3.2 Mean-field theory, DLA and average shapes

In the context of DLA, a mean field approach was proposed[47] shortly after the invention of the model. The description is close to the phase-field approach to diffusion-limited growth. Two fields are introduced, the diffusing field ϕ and the cluster density ρ. They satisfy

$$\begin{aligned} \nabla^2\phi &= \phi\ (\rho + a^2\nabla^2\rho) \\ \partial_t\rho &= \phi\ (\rho + a^2\nabla^2\rho) \end{aligned} \tag{3.12}$$

The first equation is similar to (1.5) and (1.7). When the density vanishes ϕ obeys Laplace equation. When the density is non-zero (the diffusing particles are absorbed on the aggregate), ϕ tends to zero (on a length scale proportional to $1/\sqrt{\rho}$). The second equation replaces (1.6); a particle sticks at a site if it is empty and if one of its neighbour already belongs to the aggregate. The term $(\rho + a^2\nabla^2\rho)$ comes from an heuristic linearization of this condition $[1-\rho(x)](1-\Pi_\delta[1-\rho(x+\delta)])$.

This mean field theory enjoyed an initial success when radially-symmetric solutions were computed[48]. For such solutions, it was found that the density $\rho(r)$ was inversely proportional to the distance to the center of the aggregate, $\rho(r) \sim 1/r$. This was interpreted as indicating a fractal dimension $D = d - 1$, a quite reasonable result for high dimensions. It was, however, quickly realized that the radially symmetric shapes are unstable[49] in close similarity with the classic Mullins-Sekerka instability of a sharp interface (see section 1.2). As a consequence a perturbation expansion around these solutions seems seriously compromised and their status quite unclear.

One consequence of the Mullins-Sekerka instability is that stable non-trivial propagating shapes exist when surface tension is anisotropic, as recalled in the previous sections, or, in the isotropic case when the geometry is restricted to a strip[6] or to a wedge[43]. It may therefore be thought that this would also be a consequence of equations (3.12). In an attempt to determine which kind of patterns this would describe, many diffusion-limited aggregates were grown in a strip geometry (with reflecting side boundary conditions)[50]. The average aggregate local density, obtained by superimposing the different aggregates, is peaked around the strip center and quite reminiscent of the classical Saffman-Taylor finger shape.

Can this be described by solving the equations (3.12) in a strip geometry? Surprisingly, the answer is negative. The reason is that these equations have a pathological singularity in finite time in this linear geometry[51]. One simple way of seeing it, is to first consider a one dimensional-geometry (along x) and remark that, when the density is negligible, $\phi(x) = x$. Then, an exact solution for the density field is

$$\rho(x) = \rho_0 \ \exp(-x\alpha_0(t)), \quad \frac{d\alpha_0}{dt} = -(\alpha_0 + a^2\alpha_0^2) \tag{3.13}$$

which obviously becomes flat in finite time. Of course, before that the approximation of a negligible density field fails. It becomes strongly inaccurate when there is a point x such that $x > 1/\sqrt{\rho(x)}$ since the origin is then completely screened. This can be taken into account by using (3.13) only until the first time t_1 when such a point x_1 appears. One can then approximate the field by $\phi(x) = 0$ if $x < x_1$, $\phi(x) = x - x_1$ if $x > x_1$. An equation similar to (3.13) holds for $t > t_1$ with x_1 and t_1 as new space and time origin and $\rho(x) = \rho_1 \exp -(x - x_1)\alpha_0(t_1)$, $x > x_1$ as new initial condition. This new approximation fails again at a time t_2 where the process can again be repeated. The outcome of this succession of approximations is to preserve the fact that the aggregate reaches $x = \infty$ in a finite time but the flat density profile is replaced by a density decreasing like $1/x^2$. Moving from a one dimensional to a strip geometry does not change anything since the fastest growing mode (a simple cosine mode in the transverse direction) obeys essentially one-dimensional equations in the low density front part.

At this stage, new equations seem required. A rather conservative modification has been proposed in ref.[52]. The idea is that the unphysical singularity in finite time and infinite front velocity propagation occur because the $\rho = 0$ medium is linearly unstable in eq.(3.12) whereas in reality a small but finite density is required to promote growth. This can be heuristically be taken into account by replacing the r.h.s. of (3.12) by $(\rho^\gamma + a^2\nabla^2\rho)$ with $\gamma > 1$. When these new equations are solved, results in good agreement with the numerical simulations of[50] are obtained. The real meaning of these results is of course subject to some debate since with $\gamma > 1$ a new length scale is introduced and it seems necessary to take the limit $\gamma \to 1$ at some stage. In a recent interesting work, the authors argue that a similar modification follows naturally from a careful derivation[4] of eq.(3.12). It remains to be seen whether this can give rise to a satisfactory statistical theory of these complex patterns.

3.3 η-models, transitions and Laplacian walks

A generalized version of DLA has been proposed in[53] to model dielectric breakdown. It is defined by assigning to any empty site of the cluster boundary a growth probability proportional to $\phi(x)^\eta$, ϕ on the cluster itself being equal to zero.

An interesting simpler related model is given by the 'Laplacian random walks'[54]. The growth rules are similar but branching is forbidden. Growth is only allowed in the empty sites neighbours of the tip of the growing linear object (again with probability proportional to ϕ^η). Even in this simpler setting, very few properties are known precisely. The case $\eta = 1$ is equivalent to a model of self-avoiding walks obtained by erasing loops from the path of simple random walks as soon as they appear[55]. Using this equivalence and other ingenious mappings, it has been shown[56] that the fractal dimension $D(\eta = 1)$ of Laplacian random walks for $\eta = 1$ is $5/4$, the fractal dimension of chemical paths on random spanning trees. Numerical enumerations of short walks[54] indicates that $D(\eta)$ tends quickly to one as η increases but the behaviour of $D(\eta)$ as $\eta \to \infty$ has not been determined precisely. It does not even seem to be known whether D tends asymptotically to one when $\eta \to \infty$ or if it reaches one at a finite value of η.

In section 2.5, the competition between different growing branches has been addressed using a simplified needle picture. In this model, for $\eta > 6$, three needles cannot grow simultaneously. It can be wondered whether a similar property hold for the full η-model for η larger than a critical value η_c. The resulting aggregate would then be effectively linear and could be described on a coarse-grained scale by Laplacian random walks. In order to test this hypothesis, η-aggregates were generated[57] for $1 \leq \eta \leq 8$. For $\eta \geq 6$, the fractal dimension is not distinguishable from 1 and the aggregates are effectively branchless. However, the simulated aggregate sizes are rather small for large η. So, the possibility that for $\eta > \eta_c \approx 6$ the η-model reduces to Laplacian walks is certainly compatible with the simulation results but it is quite difficult to exclude finite size effects. It appears also quite possible that the fractal dimension becomes strictly equal to 1 for $\eta > \eta'_c$ (η'_c being possibly different from η_c).

It may be a way to assess the advancement of theories of growing Laplacian fractals that no precise answer to these questions is obtained. This shows that much remains to be understood . We hope that the reader will find this a stimulating challenge.

Acknowledgements

I am grateful to B. Derrida, A. Mc Kane and E. Speer for inviting me to attend the very stimulating "Cellular automata, aggregation and growth" workshop at the Isaac Newton Institute. I would also like to thank M. R. E. Proctor and the nonlinear dynamics group at D A M T P, Cambridge, for their kind hospitality during the writing of these notes and J. Vannimenus for his careful reading of the manuscript.

REFERENCES

1. Cross M., Hohenberg P. C. (1993) Rev. Mod. Phys. **65**,851
2. Langer J. (1980), Rev. Mod. Phys.**52**, 1
3. Kessler D., Koplik J., Levine H. (1988), Adv. Phys. **37** 255 ; Brener E., Melnikov V.I., (1991), Adv. Phys. **40**, 53-97.
4. An interesting collection of reprints can be found in Pelcé P.,(1988), *Dynamics of Curved Fronts* (Academic Press, Orlando, FL)
5. Vicsék T. (1989) *Fractal Growth Phenomena* (World Scientific, Singapore)
6. Saffman P.G., Taylor G.I., Proc. R. Soc. **A 245** 312 (1958)).
7. The reader is strongly encouraged to consult Y. Couder's lectures at this school where many experimental examples are described. The present notes can in fact be thought of as theoretical attempts to understand the experimental results described there.
8. Mullins W. W., Sekerka R. F., J. Appl. Phys. **3** 444 (1964).
9. Ivantsov G. P., Dokl. Akad. Nauk. SSSR **58** 567 (1947) reprinted in[4].
10. Pelcé P., Pomeau Y. (1986) Stud. Appl. Math. **74** 245
11. In ref.[10] the parameter $C = 4/\sigma$ is used instead.
12. This may be seen as follows[6]. Let the interface be parametrized by its curvilinear abscissa s. On one hand, $\frac{\partial y}{\partial s} = -\cos\theta$. On the other hand, $\frac{\partial \phi}{\partial n} = \cos(\theta) = -\frac{\partial \psi}{\partial s}$ from eq(1.6) and the fact that $\phi + i\psi$ is an analytical function. Comparing the two equations, one readily obtains $\psi = y$ on the interface with suitable choices of origin.
13. McLean J. W., Saffman P. G. (1981), J. Fluid Mech. **102**, 455–469.

14. Vanden-Broeck J. M. (1983), Phys. Fluid **26**, 2033–2034.
15. Kruskal M., Segur H. (1991), Stud. Appl. Math. **85**, 129–181 and references therein.
16. Segur H., Tanveer S., Levine H., eds. (1991) *Asymptotics beyond all orders* (Plenum Press, New York)
17. Hakim V. (1991), p. 15 in ref.[16]
18. Combescot R., et al (1988), Phys. Rev. A **37**, 1270-1283.
19. Ben Amar M., Pomeau Y. (1986), Europhys. Lett. **2**, 307.
20. Dorsey A.T., Martin O.,(1987) Phys. Rev. A **35**, 3989.
21. Bensimon D., Pelcé P., Shraiman B. S., (1987) J. Phys. France **48**, 2081
22. Tanveer S., (1987) Phys. Fluids **30**, 2318
23. Kessler D. A., Levine H. (1986), Phys. Rev. A**33**, 2632
24. Maurer J., et al (1988) Europhys. Lett. **8** 67
25. Herring C. (1951), Phys. Rev. **82** 87 and in *The Physics of Powder Metallurgy* p.463 W.E. Kingston ed. (Mc Graw-Hill, N.Y., 1951)
26. Taylor J. E. (1992) Act. Metall. Mater. **40** 1475 and references therein.
27. Ben Amar M., Pomeau Y. (1988), Europhys. Lett. **6** 609
28. Adda-Bedia M., Hakim V., (1994) J. Phys. I France **4**, 383
29. N.I. Muskelishvilii *Singular Integral Equations* (Nordhoff, Groningen, 1953)
30. An opposite sign convention on the u field is taken in[28].
31. Adda-Bedia M., Ben Amar M., (to be published)
32. Almgren R., Dai W.-S., Hakim V., (1993) Phys. Rev. Lett.**71**, 3461
33. Eckmann J. P. et al, (1989) Phys. Rev. A**39**, 3185
34. Brener E., (1993) Phys. Rev. Lett.**71**, 3653
35. Derrida B., Hakim V., (1992) Phys. Rev. A **45**, 8759 and references therein.
36. Adda-Bedia M.,(1994) Thesis, Université Paris VI ; Krug J. et al (1993) Europhys. Lett. **24**, 527 and references therein.
37. see e.g. ref.[50]. However, the regularisations of short wavelengths in both cases are quite different and, although the equations are similar, that may play an important role, as shown by the anisotropic case (see section . Also, it is not clear (at least to the present author) whether a fractal would be obtained if the deterministic equations (1.5- 1.7) were integrated starting from a random initial condition, but with no added noise during the growth.
38. Several other approaches have been proposed. Two particularly interesting ones are Cafiero R., Pietronero L., Vespignani R. Phys. Rev. Lett.**70**, 3989 and references therein, where a quite successful real-space-renormalization-group-like scheme is developed, and Halsey T. C. (1994) Phys. Rev. Lett.**72**, 1228, where a picture of the dynamics based on the competition between two growing branches is proposed. The reader should consult these references for more information.
39. Galin L., (1945) Dok. Akad. Nauk. SSSR **47**, 246
40. Shraiman B. I., Bensimon D., (1984) Phys. Rev. A**30**, 2840
41. Howison S., (1986) SIAM J. Appl. Math. **46**, 20; J. Fluid Mech. **167**, 439
42. Richardson S., (1972) J. Fluid Mech. **56**, 609
43. Thomé H. et al, (1989) Phys. Fluid A **1**, 224.
44. Surface tension regularises the short wavelength dynamics of the Mullins-Sekerka instability and prevents singularity formation on the interface as a consequence. It can however drive a completely different kind of interface singular behaviour resulting from the merging and reconnection of different interface parts. This has recently been studied in Dupont T. P. et al (1993) Phys. Rev. E **47**, 3939
45. Dai W.-S., Kadanoff L. P., Zhou S. M. (1991), Phys. Rev. A **43**, 6672
46. Tanveer S., Phil. Trans. R. Soc. Lond. A**343**, 1.
47. Witten T., Sander L. M. (1983) Phys. Rev. B**27**, 5696
48. Ball R., Nauenberg M., Witten T., (1984) Phys. Rev. A**29**, 2017
49. Nauenberg M., Sander L. M. (1984) Physica **123A**, 360
50. Arnéodo A., et al (1989) Phys. Rev. Lett.**63**, 984
51. Hakim V. (1991), in *Growth and Form* ed Ben Amar M. et al (Plenum, N.Y.)
52. Brener E., Levine H., Tu Y., (1991) Phys. Rev. Lett.**66**, 1978; Levine H., Tu Y. (1993) Phys. Rev. E**48**, 4207
53. Niemeyer L., Pietronero L., Wiesmann H. J., (1984) Phys. Rev. Lett.**52**, 1033
54. Lyklema J. W., Evertsz C., Pietronero L., (1986) Europhys. Lett. **2**, 77
55. Lawler G. F., (1987) J. Phys. A**20**, 4565
56. Majumdar S.N., (1992) Phys. Rev. Lett.**68**, 2329

57. Sánchez A. et al (1992) Physica A **191** 123 ;(1993) Phys. Rev. E**48**, 1296